

Hesitation Phenomenon in Dynamical Hysteresis

J. Zemmouri, B. Ségard, W. Sergent, and B. Macke

Laboratoire de Spectroscopie Hertzienne, Université de Lille I, 59655 Villeneuve d'Ascq, France

(Received 11 March 1992)

The effect of the sweeping velocity on the hysteresis loop of a bistable system is examined in the case where the velocity is so large that the system is prevented from undergoing any transition during the forward sweep. The experiments, made on optical and electronic devices, evidence a dramatic instability ("hesitation") of the return path of the hysteresis loop for a critical value of the sweeping velocity. The main features of this generic phenomenon are well covered by a one-dimensional analytic theory which provides scaling laws in good agreement with the observations.

PACS numbers: 64.60.Ht, 42.65.Pc

The phenomenon of hysteresis is common to various systems in physics, mechanics, chemistry, etc. We report in this Letter on new effects incidentally uncovered in the course of an experimental study of dynamical hysteresis in optical bistability. Optical bistability [1,2] provides an example of purely deterministic hysteresis, observed in the absence of fluctuations. On the other hand, hysteresis is also commonly associated with first-order phase transitions, primarily governed by fluctuations. In fact the distinction between these two types of hysteresis is not clear cut. Intrinsic fluctuations and technical noise are indeed unavoidable in bistability experiments and deterministic effects play an important role in the dynamics of first-order phase transitions. We notice in particular the current interest in the search of quasicritical phenomena near the absolute boundaries of metastability in such transitions [3]. The phenomena described hereafter, generic to deterministic bistable systems, are then expected to occur in a wider class of hysteretic systems.

To be definite we consider a bistable system whose steady-state characteristic x vs μ is an S-shaped curve as given in Fig. 1. x is the output variable and μ is one of

the external parameters controlling the system. In the absence of fluctuations, the states corresponding to the upper and lower branches of the S are strictly stable, whereas those belonging to the intermediate branch are unstable. If the control parameter μ is adiabatically swept forth and back through the bistability domain ($\mu_B < \mu < \mu_A$), the system describes an hysteresis cycle as shown in Fig. 1. In any real experiment the sweep duration τ is obviously finite and dynamical effects occur [4] even at low sweep rate because of the divergence of the evolution times in the vicinity of the turning points A and B (critical slowing down) [1,2]. The hysteresis loop actually observed depends on the sweeping velocity $v = d\mu/dt$. For moderate velocities, the clear-cut transitions AA' and BB' are generally smoothed and delayed, and the hysteresis loop widens. The first optical study of these phenomena has been made on a CO₂ laser with an intracavity saturable absorber [5], and quantitative results, including scaling laws, have been recently obtained on a bistable semiconductor laser [6] and on a passive bistable device [7]. Qualitatively different phenomena occur when the sweeping velocity becomes so large that the system may be prevented from switching up during the forward sweep although the control parameter μ goes beyond the critical value μ_A [4,8]. In this regime, so-called frustrated switching [9], we evidenced—for a particular value of the velocity—a dramatic sensitivity of the return path of the hysteresis loop to very small changes of the experimental parameters. The return path seems then to "hesitate" between quite different trajectories, a phenomenon largely overlooked in previous works.

Our first demonstration of hesitation was made in absorptive all-optical bistability. The experiments were realized at a millimetric wavelength ($\lambda = 3.5$ mm) and the experimental setup, adapted from that extensively described in Ref. [10], consisted of a 23-m-long waveguide Fabry-Pérot cavity filled with HC¹⁵N gas at low pressure. The source and the cavity were tuned to the frequency of the (J) 0-1 rotational line of HC¹⁵N which behaves then as a saturable absorber. The output variable and the control parameter were, respectively, the power transmitted by the cavity and the voltage applied to the modulator

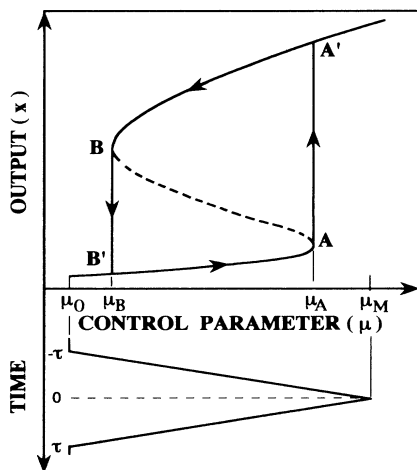


FIG. 1. Steady-state characteristic of a bistable system and standard sweeping scheme.

controlling the input power. We used a triangular voltage with equal rise and fall times (τ), according to the scheme of Fig. 1. The hysteresis loops were recorded sweep by sweep (no accumulation) and, if necessary, a dwell time was arranged between successive sweeps in order to start each sweep from equilibrium.

The recordings of Fig. 2 were obtained for a same sweeping amplitude and different sweeping durations, short enough to be in the regime of frustrated switching. For $\tau > 138 \mu\text{s}$, the return path of the hysteresis loop crosses the upper branch of the static cycle for values of the control parameter μ larger or even smaller (subcritical switching [4]) than the critical value μ_A [Figs. 2(a) and 2(b)]. For $\tau < 138 \mu\text{s}$ (not shown), the return path remains close to the lower branch. The phenomenon of hesitation occurs for $\tau = 138 \mu\text{s}$. Figures 2(c) and 2(d) show the trajectories obtained for 23 different sweeps achieved in *identical conditions*. The uncontrolled changes of the gas, source, and/or sweeping parameters from sweep to sweep are sufficient to generate quite different return paths, crossing either the upper or the intermediate branch of the steady-state characteristic. The separatrix between these two types of trajectories is obviously expected to run through the turning point B . This separatrix—analogue to those considered in Ref. [4] in a slightly different context—corresponds to a well-defined relation between the experimental parameters and the hesitation simply evidences that this relation is very critical. Its fulfillment with the required precision is then quite unlikely and this explains in particular why the

turning point B seems to be avoided by the trajectories of Figs. 2(c) and 2(d). Various experiments for different sweeping amplitudes showed that the smaller the relative overdrive, $D = (\mu_M - \mu_A) / (\mu_A - \mu_0)$, the more pronounced the phenomenon and the smaller the corresponding sweeping velocity v_c .

All the observed dynamical behaviors are well reproduced by numerical simulations using the standard ring cavity model in the plane wave and uniform field approximation [2]. In our case of purely absorptive bistability, this model involves three real dynamical variables. The calculations were made with parameters representative of the experiments, namely, $\kappa/\gamma_{\perp} = \kappa/\gamma_{\parallel} = 2.7$ and $C = 20$ in the standard notations [2]. We explored a wide range of overdrives, including situations such that $D \ll 1$, difficult to address experimentally because of the unavoidable drifts of the parameters. We found that v_c scales as $D^{3/2}$ with a precision better than 5% for $0.01 \leq D \leq 0.5$.

Complementary experiments were made with an electronic circuit designed to model the dynamical equation generic for one-dimensional bistability:

$$dx/dt = F(x, \mu) = 3x - x^3 + \mu. \quad (1)$$

The corresponding steady-state characteristic is a well-developed symmetrical S. Quite generally, the steady-state characteristic is the boundary between the regions where $dx/dt = F > 0$ or < 0 , and this simple remark suffices to explain the main features of the hysteresis loops observed in dynamical regime (Fig. 3). In the conditions of frustrated switching the forward path keeps below the S, and x and μ increase ($F > 0$, $d\mu/dt > 0$) up to the reversal point M where the sweep rate changes sign. μ then decreases whereas x continues to increase and the trajectory unavoidably crosses the S. At the crossing point, the output signal reaches its maximum ($F = 0$) and finally decreases ($F < 0$). The S is thus the locus of the maxima of the traces [11] which lie on the upper [Fig. 3(a)], intermediate [Fig. 3(c)], or lower [Fig. 3(e)] branch according to the sweep rate. Let us notice that the negative-slope unstable branch can in particular be mapped out from a suitable set of traces generated by varying the sweep rate and eventually the overdrive D . Small D indeed allow us to obtain clear-cut maxima, but larger D may be required to map the region close to the turning point B when the hesitation phenomenon itself prevents these points from being attained, as evidenced in the optical experiments [Fig. 2(d)]. On the contrary, owing to a much lower level of fluctuations, this region, including B itself [Fig. 3(b)], is attained even for fairly small D with our electronic device in the hesitation regime [Fig. 3(c)]. The perfect control of the parameters allowed us to also study experimentally the dependence of the critical velocity v_c on the overdrive D . We found again that v_c scales as $D^{3/2}$, a law fulfilled with a precision of 3% for D ranging from 0.03 to 0.5. We finally examined the effect of the fluctuations, simulated by add-

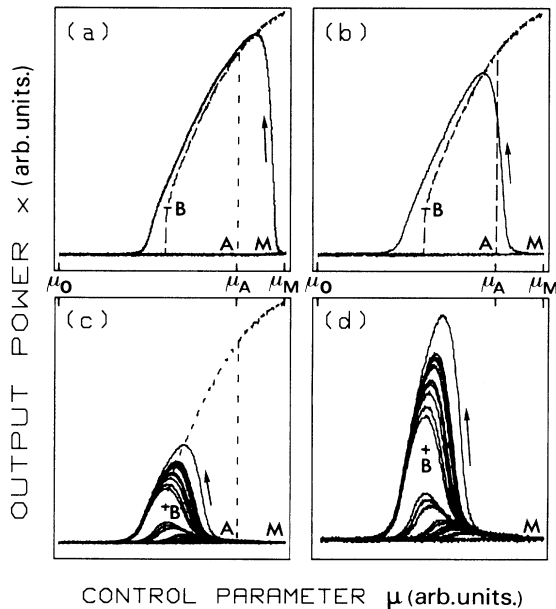


FIG. 2. Dynamical hysteresis loops in absorptive optical bistability. Sweeping duration $\tau =$ (a) 250, (b) 167, and (c) 138 μs . (d) Same as (c) with a vertical magnification $\times 2.3$. The static loop (dashed line) is given for reference.

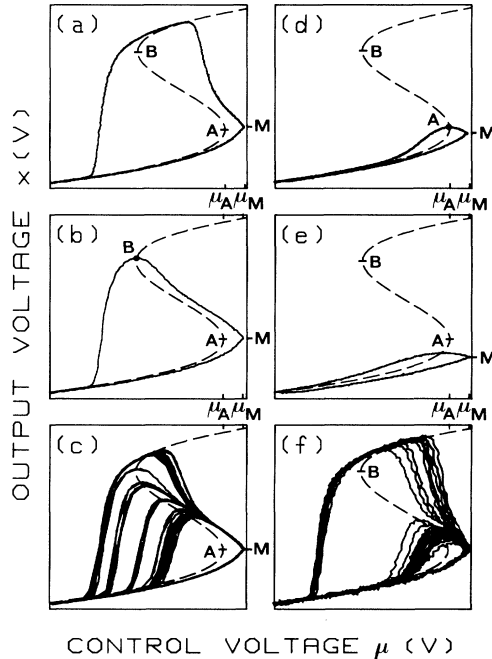


FIG. 3. Dynamical hysteresis loops in one-dimensional bistability for $\tau =$ (a) 367, (b), (c) 350, (d) 193, and (e) 25 μs . (f) Same as (c) with a rms voltage of noise equal to 30% of the overdrive added to the control parameter. (b) is extracted from the family (c). The steady-state characteristic (dashed line) is given for reference. Time constant of the circuit: 48 μs . The frameworks correspond to $-6 < \mu < +3$ V and $-2.5 < x < +2.2$ V.

ing a white noise to the control voltage. Although deterministic, the hesitation phenomenon resists the fluctuations. For rms voltages of noise as large as 30% of the overdrive, the critical velocity is not significantly modified but, as expected, the trajectories depart sooner from the separatrix in the presence of noise and avoid the turning point B [Fig. 3(f)], as in the optical experiments.

The hesitation is a quite general phenomenon and occurs whenever a bistable system, prepared in a state M such that $\mu_M - \mu_A$ is a small positive quantity and x_M is comparable to or smaller than x_A , is subjected to a negative sweep. We studied the influence of x_M by using an asymmetric triangular sweep allowing us to prescribe any position to the reversal point independently of the negative sweep rate. We only note here that reducing x_M for a given overdrive (as reducing the overdrive for a given x_M) gets the "hesitating" return paths to run closer and closer to A and to diverge from each other sooner and sooner after their passage close to A . This naturally leads to the conjecture that the hesitation mainly originates from the dynamics in the vicinity of this turning point. In this region the steady-state characteristic of any one-dimensional bistable system can be approximated by a parabola [12] and the dynamical equation reads

$$dx/dt = \alpha(\mu - \mu_A) + \beta(x - x_A)^2. \quad (2)$$

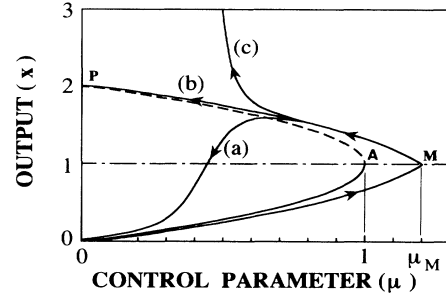


FIG. 4. Parabolic model: (a) $\Delta\mu = -10^{-4}$, (b) separatrix, (c) $\Delta\mu = +10^{-4}$.

A similar equation is expected to hold for the n -dimensional systems, the dynamics of which is generally dominated by a single master variable in the vicinity of a turning point [4]. The main features of the hesitation are indeed well reproduced by this so-called parabolic approximation. An elementary dimensional analysis of Eq. (2) first shows that the critical velocity v_c corresponding to a state M such that $x_M = x_A$ may only scale as $\alpha^{1/2}\beta^{1/2}(\mu_M - \mu_A)^{3/2}$, that is, as $D^{3/2}$, in agreement with our observations. In fact, Eq. (2) can be analytically integrated in terms of the Airy functions when the sweep is linear [13]. The equation of the trajectories in the plane (μ, x) reads

$$x = 1 - v^{1/3} \{ \text{Ai}'(\xi) + k \text{Bi}'(\xi) \} / \{ \text{Ai}(\xi) + k \text{Bi}(\xi) \}, \quad (3)$$

with $\xi = v^{-2/3}(1 - \mu)$. All the quantities introduced in Eq. (3) are dimensionless and x and μ have been suitably shifted and scaled so that the steady-state parabola looks as shown in Fig. 4. Note that the lower and upper branches of the parabola are stable and unstable, respectively, and that the second stable branch and the turning point B are at infinity in this model. The separatrix of the hesitation, now defined as separating the trajectories diverging up or falling down, must bring the bistability on the unstable branch of the parabola at the end of the negative sweep ($\mu = 0$), that is, P (Fig. 4). This condition fixes the integration constant $k(v_c)$ and then the separatrix $C(v_c)$ for a prescribed critical velocity ($v = -v_c$). Conversely, if the negative sweep rate starts from any point M of $C(v_c)$, v_c and the part $\mu < \mu_M$ of $C(v_c)$ will be the critical velocity and the separatrix of the hesitation, respectively. A remarkable point of $C(v_c)$ is its intersection with the parabola axis ($x = x_A = 1$) and it is quite convenient to characterize $C(v_c)$ by the corresponding overdrive D . Putting $x = 1$ in Eq. (3), we get

$$\text{Ai}'(-v_c^{-2/3}D) + k(v_c)\text{Bi}'(-v_c^{-2/3}D) = 0. \quad (4)$$

For $v_c \ll 1$, $k(v_c) \cong 0$ and Eq. (4) reduces to $v_c = (D/|a_1'|)^{3/2}$, where $a_1' = -1.019$ is the first zero of $\text{Ai}'(\xi)$. As expected, v_c scales as $D^{3/2}$. The assumption $v_c \ll 1$ implies $D \ll 1$, but a complete calculation shows that the precision is better than 1% up to $D = 1$. The previous re-

sults are general and directly apply to the sweeping scheme of Fig. 1. The symmetry of the sweep and that of the initial and final states (Fig. 4) indeed imply that the separatrix and the corresponding forth trace are symmetric with respect to the parabola axis [see Eq. (3)] and thus that the reversal point M has the same ordinate as the turning point A , as clearly evidenced in our experiments [Figs. 3(b), 3(c), and 3(f)]. The critical character of the hesitation is also well described by the parabolic model. To be definite, let us again consider the sweeping scheme of Fig. 1 in the limit $D \ll 1$ ($k \cong 0$ for the separatrix) and examine the effect of a very small change $\Delta\mu$ of the sweeping amplitude ($\Delta\mu \ll D$). The reversal point is then invisibly displaced on the forth path. For $\Delta\mu > 0$, k takes a very small negative value and the return path, first undistinguishable from the separatrix, leaves it upwards when $\text{Bi}(\xi)$ becomes large enough so that the first zero of $\text{Ai}(\xi) + k \text{Bi}(\xi)$ is approached [see Eq. (3)]. On the contrary, the system relaxes down if $\Delta\mu < 0$ (Fig. 4). The deviation Δx of the return path from the separatrix can be explicitly calculated at the first order in $\Delta\mu$:

$$\Delta x(\mu) = g \Delta\mu D^{-1/2} \text{Ai}^{-2}(\xi), \quad (5)$$

with $g = 2|a_1'|^{1/2} \text{Ai}(a_1') |\text{Ai}''(a_1')| \cong 0.59$ and $\xi = |a_1'| (1 - \mu)/D$, the velocity being eliminated by means of Eq. (4). A reasonable estimate of Δx in the region $\mu < 1 - D$ is given by the asymptotic expansion of $\text{Ai}(\xi)$:

$$\Delta x(\mu) = 4\pi g \Delta\mu (\xi/D)^{1/2} \exp(4\xi^{3/2}/3). \quad (6)$$

The "superexponential" divergence of Δx for $\xi > 1$ explains why very small changes of the sweeping amplitude lead to quite different trajectories (Fig. 4), especially when the reversal point M approaches the turning point A ($\xi \sim 1/D$). Equation (6) also shows that reducing $\Delta\mu$

shifts the manifestation of the divergence towards lower μ and makes this divergence more abrupt [$\xi \sim (1 - \mu)$].

We thank N. E. Fettohi for his assistance in the experiments and P. Mandel for a helpful discussion. This work was supported by the Commission of the European Community (Contract No. SCI CT90-0478). The Laboratoire de Spectroscopie Hertzienne is "Unité de Recherche Associée au CNRS."

-
- [1] H. M. Gibbs, *Optical Bistability: Controlling Light with Light* (Academic, Orlando, 1985).
 - [2] L. A. Lugiato, in *Progress in Optics*, edited by E. Wolf (North-Holland, Amsterdam, 1984), Vol. 21, pp. 69-216.
 - [3] K. Binder, *Rep. Prog. Phys.* **50**, 783 (1987).
 - [4] T. Erneux and P. Mandel, *Phys. Rev. A* **28**, 896 (1983).
 - [5] P. Glorieux and D. Dangoisse, *IEEE J. Quantum Electron.* **21**, 1486 (1985).
 - [6] P. Jung, G. Gray, R. Roy, and P. Mandel, *Phys. Rev. Lett.* **65**, 1873 (1990).
 - [7] J. Grohs, H. Ibler, and C. Klingshirn, *Opt. Commun.* **86**, 183 (1991).
 - [8] P. Mandel and T. Erneux, *Opt. Commun.* **44**, 55 (1982).
 - [9] F. Mitschke, C. Boden, W. Lange, and P. Mandel, *Opt. Commun.* **71**, 385 (1989); J. Y. Gao, G. X. Jin, J. W. Sun, X. Z. Guo, Z. R. Shen, and N. B. Abraham, *Opt. Commun.* **74**, 409 (1990).
 - [10] B. Ségard, B. Macke, L. A. Lugiato, F. Prati, and M. Brambilla, *Phys. Rev. A* **39**, 703 (1989).
 - [11] The examination of Fig. 2 and further computer simulations show that this property, specific to the one-dimensional systems, remains valid for bistable systems of larger dimension in the limit $D \ll 1$.
 - [12] P. Mandel, *Opt. Commun.* **55**, 293 (1985).
 - [13] P. Mandel, in *Frontiers in Quantum Optics*, edited by E. R. Pike and S. Sarkar (Adam Hilger, Bristol, 1986), pp. 430-452.